Presented at the 25th European PV Solar Energy Conference and Exhibition, 6-10 September 2010, Valencia, Spain

FRONT SURFACE PASSIVATION FOR INDUSTRIAL-TYPE SOLAR CELLS BY SILICON OXYNITRIDE – SILICON NITRIDE STACKS

C. Schwab, M. Hofmann, J. Rentsch, R. Preu
Fraunhofer Institute for Solar Energy Systems (ISE),
Heidenhofstrasse 2, D-79110 Freiburg, Germany

ABSTRACT: The ongoing reduction of wafer thickness and new solar cell concepts like selective emitters which make use of lowly doped emitters lead to the need for an improved front surface passivation of n-type emitters. Within this study a newly developed passivation stack system consisting of a bottom silicon oxynitride layer and a silicon nitiride capping layer for the front side phosphorous emitter of crystalline silicon solar cells is presented. The stack layers are deposited by an industrial-type plasma-enhanced chemical vapour deposition system. It is shown that the stack is firing stable and that the surface passivation can be improved compared to a single layer silicon nitride antireflection coating by using the developed double-layer system. On the other hand the used silicon oxynitride shows a non-negligible light absorption leading to a reduced short-circuit current density. The overall effect on the performance of a solar cell and a solar module is estimated and illustrates that especially the solar module performance can benefit from the passivation stack.
Keywords: PECVD, passivation, silicon oxynitride

1 INTRODUCTION

Solar cells with a selective emitter structure make use of a lowly doped phosphorus emitter in the non contacted area. Such a lowly doped emitter enables a higher influence of the emitter passivation on the solar cell performance [1].

The standard used for emitter passivation and antireflection coating of crystalline silicon solar cells in photovoltaic industry is a 70 nm-thick amorphous silicon nitride layer (in short SiN). Such a SiN passivation has been investigated in detail by Kerr [2] and Lenkeit [3].

Different double layer passivation systems (also called stacks) for the front side consisting of a thin amorphous silicon bottom layer and a silicon nitride capping layer [4, 5] or two different silicon nitride films [6] were studied recently. Also some research was done lately on double layer antireflection coatings consisting of a silicon nitride bottom layer and an on-top silicon oxide [7] or a silicon nitride bottom layer and an on-top silicon oxynitride [8].

A new passivation stack for the front side phosphorous emitter of crystalline silicon solar cells is presented in this work. The stack consists of an ultrathin (8 to 9 nm) amorphous silicon- and hydrogen-rich silicon oxynitride bottom layer (in short SiriON) and a SiN (70 nm) layer on top. Similar stacks used as rear surface passivation showed excellent results [9, 10].

2 EXPERIMENTAL DETAILS

Stack systems of ultrathin (5 to 20 nm) layers of silicon oxynitride covered by an amorphous silicon nitride (70 nm) were deposited with an industrially compatible inline PECVD (plasma-enhanced chemical vapour deposition) system (Roth&Rau SiNA). Thus the newly developed process can be directly transferred to an industrial production environment. The plasma is excited by 2.45 GHz microwave pulses coupled into the reaction chamber via a linear antenna. A deposition temperature of 400°C and a chamber pressure of 0.1 mbar were adjusted for the layer deposition. A mixture of the reactant gases nitrous oxide (N_2O), monosilane (SiH_4) and hydrogen (H_2) was used for the SiriON layer deposition. For the SiN layer deposition we used the reactant gases SiH_4 and ammonia (NH_3). Both PECVD processes used for the deposition of the stack can possibly be realized without breaking the vacuum by using adjacent reaction chambers.

Effective charge carrier lifetimes were evaluated on symmetrically passivated lifetime samples using the quasi-steady-state photoconductance technique (QSSPC) [11]. For the measurement we used a WCT-100 tool by Sinton Consulting. We used p-type (boron-doped) float-zone (FZ) silicon with a resistivity of 1 Ω cm, a crystal orientation of (100) and a thickness of 250 µm as bulk material. Prior to the layer deposition a wet chemical surface cleaning consisting of a HNO_3 treatment and a short dip in diluted HF was performed. The lifetimes are compared before and after a high-temperature step (800 °C), simulating thereby the contact firing of screen-printed contacts. The results are compared to reference samples coated with the industrial standard front surface passivation and anti-reflection coating of 70 nm SiN.

3 RESULTS

3.1 Lifetime samples with shiny etched surfaces

In a first experiment we deposited stacks with varying SiriON thickness on substrates with shiny etched surfaces and a deep $POCl_3$ emitter (E3) on both sides. The emitter parameters are shown in table 1.

The layer thicknesses were determined by spectroscopic ellipsometry using a J.A. Woolam M-2000 tool.

Table 1: Parameters of the used emitters.

Name	Sheet Resistance (Ω/sq.)	Phosphorous Surface Concentration (atoms/cm^3)	Depth (µm)
E1	75	$4.8x10^{20}$	0.34
E2	118	$6.7x10^{20}$	0.24
E3	129	$8.2x10^{18}$	0.83

The effective minority carrier lifetime τ_{eff} measured by QSSPC was evaluated at a carrier injection density of $\Delta n = 1x10^{15}$ cm^{-3}. The τ_{eff}-values measured before (hollow symbols) and after (solid symbols) firing are shown in Figure 1. The solid lines represent the lifetime of the reference sample coated with 70 nm SiN. For all used passivation layers the quality of the passivation is improved due to the high temperature treatment.

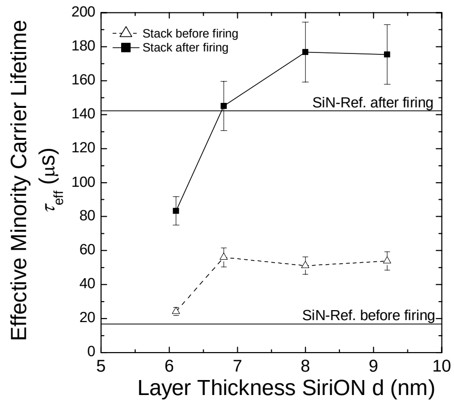

Figure 1: Effective minority carrier lifetime before and after firing plotted against the layer thickness of the different passivation stacks. The straight lines indicate the values of the reference coated with 70 nm SiN. The samples had shiny etched surfaces and a deep $POCl_3$ emitter (E3).

The QSSPC measurement permits the determination of the dark saturation current density J_{0e} and thereby the implied open-circuit voltage $V_{OC,impl}$. Therefore we used the following equations [12, 13]:

$$J_{0e} = \frac{qn_i^2}{N_{dot} + \Delta n} \times \frac{W}{2} \left[\left(\frac{1}{\tau_{eff}} - \frac{1}{\tau_{bulk}} \right)^{-1} - \frac{W^2}{D\pi^2} \right]^{-1} \quad (1)$$

$$V_{OC,impl} = V_{th} \ln \left(\frac{J_{SC}}{J_{0e}} + 1 \right) \quad (2)$$

For the determination of the Auger-limited bulk lifetime τ_{bulk} we used the Auger recombination model of Kerr [14]. The remaining parameters in equation (1) and (2) are the intrinsic carrier concentration $n_i = 9.14x10^9$ cm^{-3} (at 25 °C, according to Sproul [15]), the doping density $N_{dot} = 1.5x10^{16}$ cm^{-3}, the sample thickness $W = 250$ µm, the diffusion constant $D = 27$ cm²/s and the thermal voltage $V_{th} = 25.7$ mV (at 25 °C). We assumed an uncertainty of 10% on the values of J_{0e}, whereby the uncertainty of $V_{OC,impl}$ is also determined. Furthermore we used a short-circuit current density J_{SC} of 35 mA/cm² in equation (2).

The values of J_{0e} and $V_{OC,impl}$ after firing are shown in Figure 2. The straight and dashed lines are presenting the value of the reference. Figure 1 as well as Figure 2 show the improved passivation quality by the stack for a SiriON layer-thickness above 7 nm.

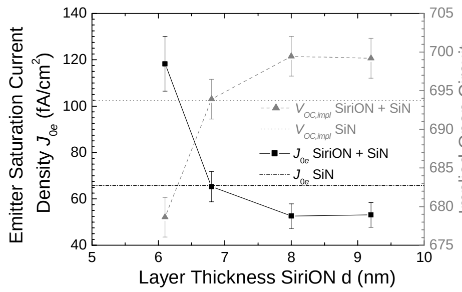

Figure 2: Values of J_{0e} and $V_{OC,impl}$ after firing plotted against the SiriON layer thickness. The values of J_{0e} and $V_{OC,impl}$ were provided by measuring the effective minority carrier lifetime by QSSPC and using equation (1) and (2). The straight and the dashed line are representing the values of J_{0e} and $V_{OC,impl}$ of the reference coated with 70 nm SiN. The samples had shiny etched surfaces and a deep $POCl_3$ emitter (E3).

3.2 Ray-tracing simulations with SUNRAYS

The optical constants of the SiriON layer were determined by spectroscopic ellipsometry and showed light absorption for wavelengths up to 580 nm.

The resulting maximal achievable short-circuit current density $J_{SC,max}$, which is the the maximum current density provided by illumination with the AM 1.5G spectrum J_{illum}.reduced by the parasitic absorption current density J_{abs} in the passivation layer and the reflected current density J_{refl} (see equation 3) was simulated using the software "SUNRAYS" [16] for the different layer thicknesses.

$$J_{SC,max} = J_{illum} - J_{refl} - J_{abs} \quad (3)$$

We calculated $J_{SC,max}$ for a solar cell with a textured surface as well as for a textured surface embedded in a photovoltaic module.

For the calculation with textured surfaces we used a 240 µm-thick silicon substrate with 7 µm-high pyramids and total reflectance on the rear side. For the solar module calculation we embedded the textured cell in a 3 mm-thick solar glass and a 0.5 mm-thick EVA foil. The optical constants of the different passivation layers were provided by spectroscopic ellipsometry measurements. The optical constants of the solar module materials were provided by the module technology centre of Fraunhofer ISE. We defined our new stack system as anti-reflection coating and varied the SiriON-thickness between 0 nm and 12 nm. The thickness of the SiN capping layer was kept constant at 70 nm. So the 0 nm SiriON stack serves as the single layer SiN reference. For illumination we used the AM 1.5G spectrum between 300 nm and 1200 nm and a radiated power of 100 mW/cm². In this wavelength range we defined sampling points with a wavelength step size of 15 nm and simulated the trace of 1000 rays in each point.

The $J_{SC,max}$-values of the cell and the module are shown in Figure 3. Due to the light absorbing module materials the values of $J_{SC,max}$ on the module level are much lower than on cell level. In both cases $J_{SC,max}$ decreases with increasing SiriON layer thickness due to the increased parasitic absorption for thicker SiriON layers. In both cases a small plateau is located around 8 nm SiriON thickness, which is assigned to a small reflection minimum.

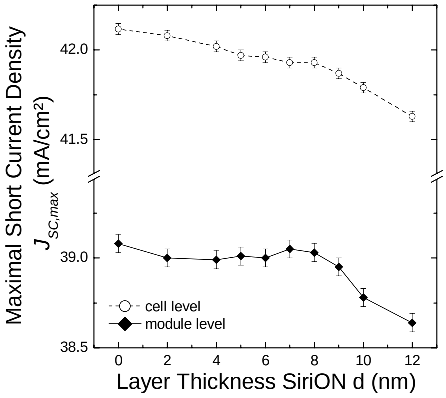

Figure 3: The maximal possible short current density $J_{SC,max}$ simulated by the raytracing software SUNRAYS for a textured solar cell coated on its front side with a passivation stack consisting of a 70 nm-thick SiN capping layer and an underlying SiriON layer with variable thickness (x-axis). Hollow symbols are representing the stand-alone solar cell, solid symbols are showing the $J_{SC,max}$-values for the same cell embedded in a typical solar module.

3.3 Lifetime samples with textured surfaces

Based on these facts we then applied a stack with a 8 nm-thick SiriON layer and a 70 nm-thick SiN layer on substrates with random-pyramid-textured surfaces. We also used two different emitters (E1 and E2, see table 1). Emitter E1 is an industrial-type emitter and emitter E2 is used for the selective emitter concept at Fraunhofer ISE [17]. Again reference samples with a single 70 nm-thick SiN layer were also processed.

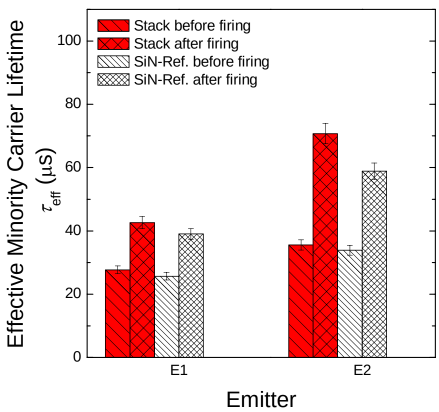

Figure 4: Effective minority carrier lifetime before and after firing measured on lifetime samples with textured surface and two different emitters.

The measured lifetimes before and after firing are shown in Figure 4. On both emitters the stack passivated samples showed higher lifetimes, but it is also clear that the level of the absolute lifetime strongly depends on the underlying emitter, which is consistent with the literature [1].

4 DISCUSSION

The investigated stack system features two basic characteristics which have a contrary impact on the solar cell performance: The maximal possible short-circuit current density of the solar cell is reduced by the light absorption in the stack, but the maximal possible open-circuit voltage is improved due to the better surface passivation of the stack.

For the estimation of the overall impact we multiplied the values of $V_{OC,impl}$ obtained from the textured lifetime samples with the values of $J_{SC,max}$ calculated by SUNRAYS. The values of this product for a stack passivation consisting of a 8 nm-thick SiriON layer and a 70 nm-thick SiN layer as well as for a single 70 nm-thick SiN layer reference are presented in Figure 5 for a solar cell and a solar module. From this it follows that especially solar modules can benefit of the new passivation stack. However, the difference between the SiN reference and the newly developed stack system is small and within the set uncertainties.

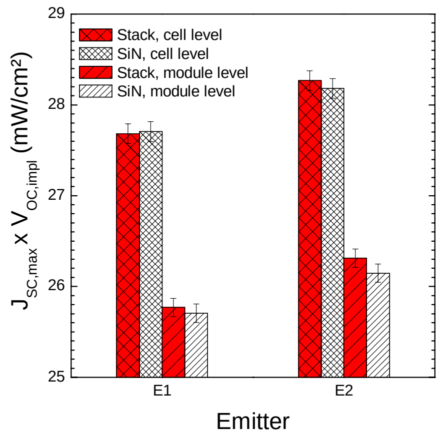

Figure 5: Values of the product $J_{SC,max}$x$V_{OC,impl}$ for a stack passivation with 8 nm SiriON and a SiN reference for a solar cell and a solar module for two different emitters.

5 SUMMARY

A PECVD-passivation stack consisting of an 8 nm-thick amorphous silicon-rich silicon oxynitride layer covered by a 70 nm-thick amorphous silicon nitride layer was developed and applied to the phosphorous emitter of a crystalline silicon solar cell. By using this stack the passivation is improved compared to a single silicon nitride coating. As it was shown a minimum film thickness of 7 nm for the silicon oxynitride is required to achieve this improvement.

The silicon oxynitride used in the stack features an enhanced light absorption, thereby reducing the short-circuit current density of a solar cell. The maximal possible short-circuit current density of a solar cell coated with the stack system was simulated using the software SUNRAYS for a single solar cell as well as for a solar cell embedded in a typical solar module. The comparison with a single silicon nitride coating showed that especially solar modules can benefit of the new passivation stack, which is based on the light-absorbing module materials, whereby the light absorption in the stack is put into perspective.
Due to the very low silicon oxynitride thickness needed and the industrial-type equipment used for the layer development, a very-high-throughput process for industrial application is already quickly implementable.

ACKNOWLEDGMENTS

This work was supported by the German Ministry for the Environment, Nature Conservation and Nuclear Safety (BMU) under contract no. 0329849B.

REFERENCES

[1] A. Cuevas, P.A. Basore, G. Giroult-Matlakowski and C. Dubois, Journal of Applied Physics 80 (1996) 3370.
[2] M.J. Kerr. Vol. PhD, pp. 228, Australian National University 2002.
[3] B. Lenkeit. PhD in Fachbereich Physik, pp. 232, Universität Hannover 2002.
[4] H. Plagwitz. PhD in Fakultät für Mathematik und Physik, pp. 157, Universität Hannover 2007.
[5] A. Richter, J. Benick, M. Hermle and S.W. Glunz, Proceedings of the 24th European Photovoltaic Solar Energy Conference, Hamburg, Germany (2009) 1534.
[6] P. Engelhart. PhD in Fakultät für Elektrotechnik und Informatik, pp. 162, Universität Hannover 2007.
[7] H. Nagel. PhD in Fachbereich Physik, pp. 258, Universität Hannover 2002.
[8] J. Dupuis, Proceedings of the 24th European Photovoltaic Solar Energy Conference, Hamburg, Germany (2009).
[9] J. Seiffe, L. Weiss, M. Hofmann, L. Gautero and J. Rentsch, Proceedings of the 23rd European Photovoltaic Solar Energy Conference, Valencia, Spain (2008) 1700.
[10] J. Seiffe, L. Gautero, M. Hofmann, J. Rentsch, R. Preu, S. Weber and R. Eichel, Journal of Applied Physics (handed in for publication 2010).
[11] R.A. Sinton and A. Cuevas, Applied Physics Letters 69 (1996) 2510.
[12] A.B. Sproul, Journal of Applied Physics 76 (1994) 2851.
[13] C. Reichel, F. Granek, J. Benick, O. Schultz-Wittmann and S.W. Glunz Progress in Photovoltaics: Research and Applications published online (2010).
[14] M.J. Kerr and A. Cuevas, Journal of Applied Physics 91 (2002) 2473.
[15] A.B. Sproul and M.A. Green, Journal of Applied Physics 73 (1993) 1214.
[16] R. Brendel, Proceedings of the 12th European Photovoltaic Solar Energy Conference, Amsterdam, The Netherlands (1994) 1339.
[17] U. Jäger, M. Okanovic, M. Hörteis, A. Grohe and R. Preu, Proceedings of the 24th European Photovoltaic Solar Energy Conference, Hamburg, Germany (2009) 1740.